

The reactions $\pi\pi \rightarrow \pi\pi$ and $\gamma\gamma \rightarrow \pi\pi$ in χ PT with an isosinglet scalar resonance

Arbin Thapaliya^{1,2} and Daniel R. Phillips²

¹*Department of Chemistry and Physics, Franklin College, Franklin, Indiana 46131 USA*

²*INPP and Department of Physics and Astronomy, Ohio University, Athens, Ohio 45701 USA*

Abstract

The lowest-lying resonance in the QCD spectrum is the 0^{++} isoscalar σ meson, also known as the $f_0(500)$. We augment SU(2) chiral perturbation theory (χ PT) by including the σ meson as an additional explicit degree of freedom, as proposed by Soto, Talavera, and Tarrús and others. In this effective field theory, denoted χ PT_S, the σ meson’s well-established mass and decay width are not sufficient to properly renormalize its self-energy. At $\mathcal{O}(p^4)$ another low-energy constant appears in the dressed σ -meson propagator; we adjust it to reproduce the isoscalar pion-pion scattering length. We compare the resulting amplitudes for the $\pi\pi \rightarrow \pi\pi$ and $\gamma\gamma \rightarrow \pi\pi$ reactions to data from threshold through the energies at which the σ -meson resonance affects observables. The leading-order (LO) $\pi\pi$ amplitude reproduces the σ -meson pole position, the isoscalar $\pi\pi$ scattering lengths and $\pi\pi$ scattering and $\gamma\gamma \rightarrow \pi\pi$ data up to $\sqrt{s} \approx 0.5$ GeV. It also yields a $\gamma\gamma \rightarrow \pi\pi$ amplitude that obeys the Ward identity. The value obtained for the π^0 polarizability is, however, only slightly larger than that obtained in standard χ PT.

1 Introduction

The spectrum of Quantum Chromodynamics (QCD) consists of several bound and resonant states with masses below 1 GeV. The lightest QCD bound states are the pseudoscalar pions, which have a special role in the theory as pseudo-Nambu-Goldstone bosons of QCD’s approximate, spontaneously-broken, chiral symmetry. The lowest-lying QCD resonance has 0^{++} quantum numbers: the same as those of the vacuum. This state, often termed the “ σ meson”, and also referred to as the $f_0(500)$, is (slightly) manifested in pion-pion scattering [1]. It has attracted much attention over many years—indeed the suggestion that the meson spectrum contains a somewhat light scalar pre-dates QCD itself [2, 3]. However, the σ meson’s vacuum quantum numbers mean it resides in the least understood sector of QCD, and only recently has a clear picture of dynamics in this channel begun to emerge.

Determinations of σ -meson parameters rely on an extrapolation of the $\pi\pi$ scattering amplitude into the complex plane: one must obtain its mass, M_σ , and width, Γ , from the position in the complex energy plane at which a pole in the $\pi\pi$ t -matrix occurs. From 1996–2010 the Particle Data Group (PDG) [4] results for the mass and decay width ranged from 400 to 1200 MeV and from 500 to 1000 MeV, respectively. These wide variations occurred because obtaining the mass, decay width, and couplings of this resonance is difficult: the resonance is very broad and can hardly be seen in the $\pi\pi$ scattering phase shifts. The standard Breit-Wigner formulation for narrow resonances is definitely not applicable in this case. The last fifteen years has seen the advent of dispersion-relation evaluations that incorporate the constraints of chiral symmetry and—in some

cases—crossing symmetry too [5, 6, 7, 8]. The results of these calculations largely agree, and the 2015 review of Peláez quotes a σ -meson pole position [1]:

$$\sqrt{s} = M_\sigma - i\Gamma/2; \quad M_\sigma = (449_{-16}^{+22}) \text{ MeV}; \quad \Gamma = (550 \pm 24) \text{ MeV}. \quad (1)$$

This result implies that QCD’s spectrum includes a scalar isosinglet state at low mass. That is in accord with a recent lattice QCD calculation by Briceño and collaborators [9]. They find that at pion masses $m_\pi \approx 400$ MeV the σ is a $\pi\pi$ bound state, but, as the quark mass in their simulation is lowered (ultimately to a smallest value of $m_\pi = 236$ MeV), this state becomes a broad resonance.

The pole position (1) is markedly lower than the scale of chiral-symmetry breaking, $\Lambda_{\chi\text{SB}}$, which is usually understood to be the rho-meson mass, or $4\pi F$, with $F = 92.419$ MeV the pion decay constant. It is also comparable to the kaon mass. This has led some authors to propose that the σ is itself a (pseudo-)Goldstone boson of QCD. Crewther and Tunstall developed an effective field theory (EFT) based on the postulated existence of a non-perturbative infra-red fixed point in the flow of the strong coupling constant α_S in three-flavor QCD, and the consequent emergence of a QCD dilation which they identified with the σ [10]. The resulting “chiral-scale perturbation theory” includes as dynamical degrees of freedom the eight Goldstone bosons of SU(3) chiral perturbation theory and the σ . In fact, for a sufficiently large number of flavors, N_f , QCD can be expected to develop an infra-red fixed point and hence a conformal symmetry at long distances. Recent lattice studies with $N_f = 8$ support this expectation [11, 12]. However, in such a theory there is neither confinement nor chiral-symmetry breaking. Golterman and Shamir examined an extension of QCD with N_f large enough that the theory is on the verge of developing an infra-red fixed point, but not so large that the theory ceases to display confinement and chiral symmetry breaking. They conjectured that dilatation symmetry is recovered in a triple limit: the chiral limit of massless quarks, the large- N_c limit (with N_f/N_c held fixed), and the limit that the number of flavors approaches the critical value for conformality. They then developed a low-energy EFT for the pions and the dilatonic meson by making an expansion in the three small parameters associated with these different aspects of conformal symmetry breaking [13].

However, it is not necessary to assume that the σ is an (approximate) QCD dilaton in order to include it as an explicit degree of freedom in the low-energy EFT. After all, that $|M_\sigma - i\Gamma/2|$ is well below $\Lambda_{\chi\text{SB}}$ is an empirical fact. This 0^{++} resonance can therefore be expected to spoil the convergence of any perturbative expansion in channels where it plays a role (cf. Ref. [14] for lattice studies of QCD-like theories where this clearly happens). This motivates augmenting standard chiral perturbation theory by the addition of a σ field, whose mass is midway between the pseudo-Goldstone-boson mass scale, m_π , and $\Lambda_{\chi\text{SB}}$. The resulting EFT has a (spontaneously and dynamically broken) $SU(2)_L \times SU(2)_R$ symmetry. It was written down by Soto, Talavera, and Tarrús in Ref. [15], who called it χPT_S . χPT_S has also been explored by Ametller and Talavera [16, 17] and Hansen *et al.* [18]. The price to be paid for not having the σ be a Goldstone boson of a QCD symmetry is that its couplings must be fixed from data: only a few are constrained by the chiral symmetry of the EFT. In contrast, in the approaches discussed in the previous paragraph many of the σ ’s couplings are fixed. However, whether those symmetry relations prevail in nature is unclear as the connection between the version of QCD we observe experimentally and the ones considered by Golterman and Shamir and Crewther and Tunstall could be regarded as tenuous.

χPT_S is, like, the linear σ model, a low-energy theory that includes as explicit degrees of freedom the pions and a scalar. The linear σ model can be recovered as a special case of χPT_S , as explained by Soto *et al.* [15] and Hansen *et al.* [18]. However, χPT_S is more general than the linear σ model, since it does not assume that there is a LO relation between M_σ and F , or (equivalently) a specific value of the $\sigma\pi\pi$ coupling. This is tied to the fact that χPT_S , unlike the linear σ model,

does not make any assumptions about the nature of the physics that generates chiral symmetry breaking at the scale $\Lambda_{\chi\text{SB}}$.

In this paper we examine the reactions $\pi\pi \rightarrow \pi\pi$ and $\gamma\gamma \rightarrow \pi\pi$, both of which couple to the 0^{++} channel in the s -channel, and both of which exhibit slow convergence when investigated in standard, two-flavor, χPT . We compare those standard χPT calculations at leading [$\mathcal{O}(p^2)$] order to χPT_S at LO: the theory with the additional scalar isoscalar degree of freedom intercalates between χPT at $\mathcal{O}(p^2)$ and χPT at $\mathcal{O}(p^4)$. We demonstrate that χPT_S naturally includes a σ meson with a large width that is, nonetheless, not prominent in the $\pi\pi$ S-wave phase shift.

Our emphasis on scattering processes takes us beyond the static properties considered in Ref. [15, 18]. The main goal in Ref. [15] was to improve extrapolations of lattice data as a function of m_π for quantities that couple to vacuum quantum numbers. (See also the more recent Ref. [19].) Both Refs. [15, 18] computed the corrections to the pion mass and decay constant, as well as the one-loop piece of the σ mass (and hence the leading contribution to the σ width) in χPT_S .

The $\gamma\gamma \rightarrow \pi\pi$ reaction and the pion vector form factor were considered by Ametller and Talavera in Ref. [16, 17]. But, as we discuss further below, they (implicitly) had a different $\sigma\pi\pi$ coupling governing the width of the σ and its decay to two pions. This allowed Ametller and Talavera to accommodate the weak impact of the σ on the $\gamma\gamma \rightarrow \pi\pi$ cross section, yet also incorporate a σ with a large width in their theory. But such a treatment is both inconsistent and unnecessary: we will show below that a proper treatment of the reaction in χPT_S obeys the Ward identity and does not require this inconsistency in the $\pi\pi$ amplitude.

Our approach also differs from these previous works in that we employ a power counting with two light scales: m_π and M_σ . The resulting hierarchy on which the EFT is built is then $m_\pi \ll M_\sigma \ll \Lambda_{\chi\text{SB}}$. A particular virtue of this hierarchy is that the loop effects that generate the σ width in the s -channel are perturbative for values of Mandelstam s that are $\sim m_\pi^2$, i.e., within the purview of the EFT but not close to M_σ^2 . However, for $s \sim M_\sigma^2$ the infra-red singularity in the (nominal) LO σ propagator mandates the resummation of the one-loop self-energy, thereby generating a width for the resonance. For the processes that we consider it is always the case that the σ pole in the t and u channels is far away, and so resummation is not necessary there. Thus the LO amplitude in our approach consists of the standard χPT $\mathcal{O}(p^2)$ interaction plus an s -channel σ pole that is enhanced near the resonance so it becomes $\mathcal{O}(p^0)$. (Away from $s \sim M_\sigma^2$ the s -channel pole is $\mathcal{O}(p^4/M_\sigma^2)$.) This LO amplitude does violate crossing symmetry, but it does so only by loop corrections that are perturbative both for $s \sim M_\sigma^2$ and in the near- and sub-threshold region where $s \sim m_\pi^2$. This same three-scale strategy has been successfully employed for the $\Delta(1232)$ resonance in the low-energy EFT of the single-baryon sector [20, 21, 22].

The rest of this paper is structured as follows: in Sec. 2 we review the Lagrangian developed in Ref. [15] (or, equivalently, the later Ref. [18]), and explain the power counting we use in this paper. In Sec. 3 we calculate the σ propagator at $\mathcal{O}(p^4)$. In Sec. 4 we employ this propagator, together with the standard mechanisms of χPT at $\mathcal{O}(p^2)$, to describe $\pi\pi$ scattering. In Sec. 5 we consider $\gamma\gamma \rightarrow \pi\pi$. We first discuss the Ward identity for this reaction, and also explain why it is important to have a consistent treatment of the σ width and the $\sigma \rightarrow \pi\pi$ vertex—something that was not achieved in Ref. [16, 17]. We then show that the good description of phase shifts in Sec. 4 carries over to a nice reproduction of the $\gamma\gamma \rightarrow \pi^0\pi^0$ cross section up to $\sqrt{s} \approx 600$ MeV. However, the relatively weak impact of the σ meson in this process also means it produces only a small increase in the pion’s dipole polarizability. This is in contrast to, e.g., the Roy equation approach of Ref. [23] where the σ pole accounts for about half of the difference between the $\mathcal{O}(p^4)$ and $\mathcal{O}(p^6)$ numbers for the π^0 ’s dipole polarizability. Sec. 6 offers our conclusions.

2 The Lagrangian and Power counting

In Ref. [15] Soto *et al.* modified the χ PT Lagrangian—which is approximately invariant under $SU(2)_L \times SU(2)_R$ transformations—to χ PT_{*S*} by including the terms containing an isosinglet scalar σ field S . (See also Ref. [24] for a chirally-symmetric Lagrangian that incorporates an explicit scalar degree of freedom) S is then a dynamical degree of freedom that is in addition to the matrix U that parameterizes the Goldstone boson fields in standard $SU(2)$ χ PT [25, 26]. In the notation of Ref. [15] the terms in the effective Lagrangian that are relevant for this study are:

$$\begin{aligned} \mathcal{L}_2^S = & \left(\frac{F^2}{4} + Fc_{1d}S + c_{2d}S^2 + \dots \right) \langle D_\mu U (D^\mu U)^\dagger \rangle + \left(\frac{F^2}{4} + c_{1m}S + c_{2m}S^2 + \dots \right) \langle \chi U^\dagger + U \chi^\dagger \rangle \\ & + \frac{1}{2} \partial_\mu S \partial^\mu S - \frac{1}{2} m_S^2 S S + f_{2p} (\partial_\mu \partial^\mu S)^2 - \frac{\lambda_3}{3!} S^3 - \frac{\lambda_4}{4!} S^4, \end{aligned} \quad (2)$$

where c_{1d} , c_{2d} , c_{1m} , c_{2m} , and f_{2p} are new low-energy constants (LECs) in the $\mathcal{O}(p^2)$ Lagrangian. In Eq. (2), $D_\mu U = \partial_\mu U - i[v_\mu, U] + i\{a_\mu, U\}$ is the chiral covariant derivative, χ represents a scalar source (and hence is where quark masses enter the theory) and the symbol $\langle \dots \rangle$ is the isospin trace of the matrix within it. The terms on the second line are the Lagrangian of the scalar S field with bare mass m_S . This Lagrangian, unlike the typical \mathcal{L} for scalar fields, contains an additional fourth-order term which is Lorentz invariant. Although this term appears only in the $\mathcal{O}(p^4)$ Lagrangian it is needed for proper renormalization of the σ -meson self-energy. In the absence of this term, the σ couples strongly to two pions, causing the bumps in the $\pi\pi \rightarrow \pi\pi$ and $\gamma\gamma \rightarrow \pi\pi$ processes to be very pronounced—something that is not seen in data.

The LEC c_{1m} must be zero at tree level (and must be additionally tuned at loop level) to stop the scalar field S mixing with the vacuum [15]. Soto *et al.* also take $\lambda_3 = \lambda_4 = 0$, in order to implement the (presumed) triviality of strongly-coupled scalar field theories in four dimensions in the EFT. Once the scalar is coupled to Goldstone bosons (e.g., through the couplings c_{1d} , c_{2d} , and c_{2m}) values of λ_3 and λ_4 of $\mathcal{O}(m_S^2/\Lambda_{\chi\text{SB}})$ and $\mathcal{O}(m_S^2/\Lambda_{\chi\text{SB}}^2)$ will be induced through renormalization of pion-loop contributions to the three- and four-scalar correlation functions. This, however, only affects Goldstone-boson reactions beyond the order to which we work here.

In χ PT_{*S*} we consider two different energy regions of interest. In the near-threshold region we have $p \sim m_\pi$ and the standard χ PT power counting: each vertex with n powers of momentum p or m_π scales as p^n and the pion propagator scales as p^{-2} . In this regime the σ propagator scales as m_S^{-2} , since p is markedly less than m_S . It therefore produces larger threshold effects than the χ PT counter terms at $\mathcal{O}(p^4)$, since m_S is taken to be $\ll \Lambda_{\chi\text{SB}}$.

But the effects of the σ are enhanced—to an effect that is nominally larger than the $\mathcal{O}(p^2)$ leading χ PT $\pi\pi$ amplitude—in the second regime where $p \sim m_S$, i.e., in the vicinity of the resonance. Here the σ propagator develops a pole. It then needs to be dressed by the inclusion of the leading [$\mathcal{O}(p^4)$] self energy, which is resummed to all orders in the s -channel via a Dyson equation. After this is done there is a (narrow) kinematic window where the $p^2 - m_{S,r}^2$ piece of the inverse σ propagator is of the same order, or smaller than, the $\mathcal{O}(p^4)$ self-energy, $\Sigma^{(4)}$. In this kinematic window the resummed σ propagator scales as p^{-4} , is enhanced, and becomes a leading-order effect.

We note that in this second, near-resonance, kinematic domain, vertices proportional to m_π^2 are suppressed compared to vertices proportional to p^2 . For example, the effect of c_{2m} in this region is suppressed by factors of m_π^2/M_σ^2 compared to corrections to the propagator proportional to s . For this reason, in what follows, we do not consider pieces of the σ self-energy that involve two vertices each $\sim m_\pi^2$. The details of the renormalization of the one-loop σ self energy by terms involving two insertions of the chiral-symmetry-breaking quantity χ that were worked out in Ref. [15] are a higher-order effect in our approach.

3 Calculation of the σ -meson self-energy

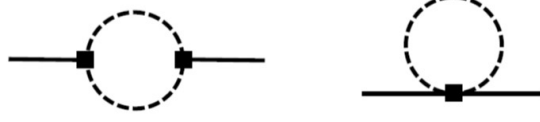


Figure 1: The self-energy diagrams of the σ meson at the one-pion-loop level, i.e. $\mathcal{O}(p^4)$. The solid (dashed) line represents the $\sigma(\pi)$ propagator. The squares indicate that the interaction appears due to the terms containing the S field in the \mathcal{L}_2^S Lagrangian. The left-hand diagram involves two insertions of c_{1d} and the right-hand one one insertion of c_{2d} or c_{2m} .

We now perform calculation of the σ -meson self-energy to $\mathcal{O}(p^4)$. Only one-loop diagrams need to be considered and the pertinent ones are shown in Fig. 1. We can express the σ self-energy in the modified minimal-subtraction (\overline{MS}) renormalization scheme as

$$\Sigma^{\overline{MS}}(s, \bar{\mu}) = \Sigma_0(\bar{\mu}) + \Sigma_1(\bar{\mu})s + \Sigma_2(\bar{\mu})s^2 + c_{1d}^2(\bar{\mu})\tilde{\Sigma}(s), \quad (3)$$

with

$$\begin{aligned} \Sigma_0(\bar{\mu}) &= -\frac{3m_\pi^4}{2\pi^2 F^2} \left[c_{1d}^2 \left\{ 2 + 3 \ln \bar{\mu}^2 \right\} + (c_{2d} - c_{2m}) \left\{ 1 + \ln \bar{\mu}^2 - \ln m_\pi^2 \right\} \right], \\ \Sigma_1(\bar{\mu}) &= -\frac{3c_{1d}^2}{2\pi^2 F^2} \int_0^1 dx \left[-2x(1-x)m_\pi^2 \left\{ 2 + 3 \ln \bar{\mu}^2 \right\} \right. \\ &\quad \left. + \left\{ \frac{1}{4}(1-2x)^2 - 2x(1-x) \right\} (-m_\pi^2) \left\{ -1 - 2 \ln \bar{\mu}^2 \right\} \right], \\ \Sigma_2(\bar{\mu}) &= -\frac{3c_{1d}^2}{2\pi^2 F^2} \int_0^1 dx \left[x^2(1-x)^2 \left\{ 2 + 3 \ln \bar{\mu}^2 \right\} \right. \\ &\quad \left. + \left\{ \frac{1}{4}(1-2x)^2 - 2x(1-x) \right\} x(1-x) \left\{ -1 - 2 \ln \bar{\mu}^2 \right\} + x^2(1-x)^2 \ln \bar{\mu}^2 \right], \\ \tilde{\Sigma}(s) &= -\frac{3}{2\pi^2 F^2} \int_0^1 dx \left[3D^2 - 2 \left\{ \frac{1}{4}(1-2x)^2 - 2x(1-x) \right\} sD + x^2(1-x)^2 \right] (-\ln(-D)), \end{aligned} \quad (4)$$

where $\bar{\mu}$ is a renormalization scale and $D = x(1-x)s - m_\pi^2 + i\epsilon$.

In Eq. (4), Σ_0 , Σ_1 , and Σ_2 are $\bar{\mu}$ -dependent whereas $\tilde{\Sigma}(s)$ is independent of $\bar{\mu}$. When Eq. (3) is combined with bare propagators and vertices the $\Sigma_0(\bar{\mu})$ -term is renormalized by $m_{S,r}^2(\bar{\mu})$ and the term linear in s by $c_{1d,r}^2(\bar{\mu})$. However, the left-hand graph in Fig. 1 is quartically divergent, and so there is also an $s^2 \ln(\bar{\mu})$ piece of the diagram that must be absorbed by a counterterm. This is done by $f_{2p}(\bar{\mu})$. We then express the dressed renormalized σ propagator as

$$i\sigma(s) = \frac{i}{s - m_{S,r}^2 - 2f_{2p,r}s^2 - c_{1d,r}^2\tilde{\Sigma}(s)}, \quad (5)$$

where the quantities with subscripts r are the $\bar{\mu}$ -independent renormalized quantities. We note that Bruns has also recently computed the σ -meson self energy, and observed the presence of the

$s^2 \ln(\mu)$ term that we found here [19]. However, he then expands the propagator around the pole, and argues that the quadratic-in- s part is irrelevant for his results. In what follows we keep $f_{2p,r}$ as a free parameter in our calculation.

This means we have three unknown parameters $m_{S,r}$, $f_{2p,r}$, and $c_{1d,r}$ that affect the σ -meson physics in our theory. These can be determined using the pole position of the σ -resonance and the experimental pion-pion scattering length $a_{\pi\pi}^{I=0}$ in the scalar-isoscalar channel. We use $M_\sigma = (449_{-16}^{+22})$ MeV and $\Gamma = (550 \pm 24)$ MeV from Ref. [1] for the σ -pole and $a_{\pi\pi}^{I=0} = 0.2210(47)(40)$ from Ref. [27]. (For details on obtaining the $\pi\pi$ amplitude that yields this scattering length from the propagator (5) see Sec. 4 below.) Here, and throughout, we take $F = 92.419$ MeV and $m_\pi = 139.57$ MeV [4]. The values of $m_{S,r}$, $f_{2p,r}$, and $c_{1d,r}$ that we then obtain are

$$m_{S,r} = 227_{-5}^{+8} \text{ MeV}; \quad c_{1d,r} = 0.205_{-0.004}^{+0.002}; \quad f_{2p,r} = (3.4_{-0.10}^{+0.05}) \times 10^{-6} \text{ MeV}^{-2}. \quad (6)$$

We note four things about these results:

1. The pole position is not $s = m_{S,r}^2$. The quadratic s -dependence $\sim f_{2p,r}$ and the s -dependence of $\tilde{\Sigma}(s)$ ultimately produce a pole at the position (1).
2. Ref. [15] noted the need for renormalization of the one-loop σ self-energy, but they set the finite part of f_{2p} to zero. (This is ultimately equivalent to Bruns removing the s^2 piece from the propagator he considers [19].) We find a finite, but natural value: $f_{2p,r} \sim 1/\Lambda_{\chi\text{SB}}^2$.
3. Our analytic result for the self-energy Σ agrees with that found in Ref. [15]. However, there is a mistake in that reference in the conversion of the self energy to the width of the σ : their analytic formula for the width is a factor of two too large. Hansen *et al.* state they reproduce the result of Soto *et al.* for the σ width in a particular limit of their (more general) calculation. Consequently our analytic formula for Γ is also a factor of two smaller than that of Ref. [18].
4. If we adopt the same strategy as Ref. [15, 19] and set $f_{2p,r} = 0$ then we need to chose $c_{1d,r} = 0.96$ in order to reproduce the σ width, i.e. $c_{1d,r}$ is a factor of $\sqrt{2}$ larger than that employed by Soto *et al.*, because our analytic expression for the width is a factor of two smaller. However, the introduction of a finite $f_{2p,r}$ ultimately permits a markedly smaller $c_{1d,r}$ to yield the observed width.

4 Pion-pion scattering at leading order in χPT_S

We now investigate the $\pi\pi \rightarrow \pi\pi$ scattering process in χPT_S from threshold through the energies at which the σ -resonance affects the phase shifts.

Consider the diagrams (i)-(iv) of Fig. 2. The thick line in diagram (i) indicates that we have resummed the σ self-energy and so are employing the propagator (5) in that diagram. In the other diagrams we employ the propagator $1/(t, u - M_\sigma^2)$, where M_σ is the real part of the σ mass. However, both these diagrams are actually negligible compared to other contributions (see below). This is in accord with the power counting, which assigns them an order p^4/M_σ^2 , where $p \sim m_\pi$ in the threshold region and $p \sim M_\sigma$ in the resonance region.

In contrast, the leading-order mechanisms are diagram (ii)—the tree-level χPT $\pi\pi$ scattering amplitude—near threshold, where it is $\mathcal{O}(p^2)$, and diagram (i)—the s -channel σ pole—in the resonance region, where it is $\mathcal{O}(p^0)$. By combining diagrams (i) and (ii) we obtain an amplitude that is leading order in both the threshold and resonance regions, and interpolates smoothly between the two.

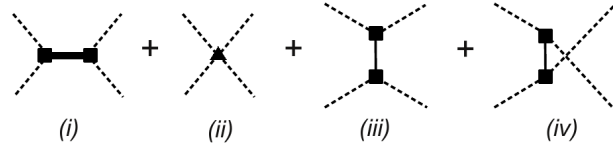


Figure 2: Tree-level diagrams contributing to $\pi\pi$ scattering in χPT_S : (i) s -channel, (ii) contact term, (iii) t -channel, and (iv) u -channel. The triangle represents the interaction from the standard χPT \mathcal{L}_2 Lagrangian. The thick solid line indicates the dressed σ propagator of Eq. (5).

Then, the isospin $I=0$ projected pion-pion scattering amplitude at LO can be written as

$$T^{I=0}(s, t, u) = \frac{1}{F^2} \left(3(s - m_\pi^2) + (t - m_\pi^2) + (u - m_\pi^2) - \frac{12c_{1d,r}^2 (s - 2m_\pi^2)^2}{s - m_{S,r}^2 - 2f_{2p,r} s^2 - c_{1d,r}^2 \tilde{\Sigma}(s)} \right). \quad (7)$$

Unlike the standard χPT amplitude, Eq. (7) does not respect crossing symmetry—even before the isospin projection is made. However, by adding graphs (iii) and (iv), with a dressed σ propagator crossing symmetry is restored. Below we also show results when this additional amplitude:

$$\Delta T^{I=0}(s, t, u) = -\frac{4}{F^2} c_{1d,r}^2 \left(\frac{(t - 2m_\pi^2)^2}{t - m_{S,r}^2 - 2f_{2p,r} t^2 - c_{1d,r}^2 \tilde{\Sigma}(t)} + \frac{(u - 2m_\pi^2)^2}{u - m_{S,r}^2 - 2f_{2p,r} u^2 - c_{1d,r}^2 \tilde{\Sigma}(u)} \right) \quad (8)$$

is included in the calculation, thus restoring crossing symmetry. We can relate the S-wave $\pi\pi$ phase shift δ_0 and $T^{I=0}$ via [28]

$$\frac{1}{|\mathbf{k}|} e^{i\delta_0} \sin \delta_0 = \frac{1}{32\pi\sqrt{s}} \int_{-1}^1 d(\cos \theta) T^{I=0}(s, \cos \theta), \quad (9)$$

where $|\mathbf{k}| = \sqrt{s - 4m_\pi^2}/2$ represents the magnitude of the center-of-mass (CM) momentum and θ the CM scattering angle.

In the left panel of Fig. 3, we plot the $\pi\pi$ scattering phase shift as predicted by the σ -meson part of the amplitude of Eqs. (7) and (8). The left plot shows the s -channel σ contribution as the solid blue curve and the combined t - and u -channel contributions as the dotted purple curve. Both these curves level off as a function of the CM energy—due to the $1/q^4$ behavior of the σ propagator at large momenta. The right graph in Fig. 3 shows the standard χPT result in the dashed purple curve and the total phase shift in the dashed green curve. We find that the size of the contributions from the σ -meson physics are generally smaller than the $\mathcal{O}(p^2)$ χPT result. Thus, although the s -channel σ -meson pole exists, it only affects the total $\pi\pi$ phase shift weakly.

In the right panel of Fig. 3 we also compare our results to $\pi\pi$ phase-shift data. The data from Ref. [29] are obtained indirectly from analysis of the reaction $\pi N \rightarrow \pi\pi N$. This has a large systematic uncertainty associated with it because one of the pions is off-shell. Also, there is a possibility that the pion and nucleon in the initial state exchange multiple pions—or another degree of freedom—instead of just one pion, thereby clouding the interpretation. Data from Ref. [27], on the other hand, are obtained by analyzing the $\pi\pi$ scattering in the final-state interactions between pions in the K_{e4} decay $K^\pm \rightarrow \pi^\pm \pi^\mp e^\pm \nu$. This graph shows that the addition of the s -channel σ -meson pole is enough to remedy the discrepancy between the $\mathcal{O}(p^2)$ χPT result and the data. Working in χPT_S and adding the s -channel σ brings the total phase shift closer to data from Ref. [29] and nicely reproduces the more reliable data from Ref. [27].

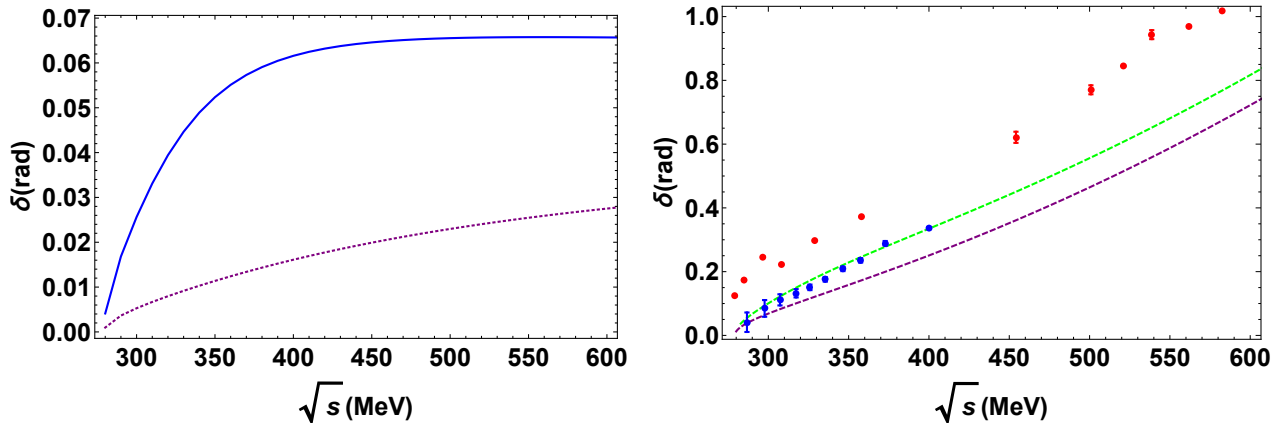


Figure 3: The $\pi\pi$ scattering phase shift as a function of the CM energy. In the left panel the solid blue (dotted purple) line represents the s - (t - and u -) channel contribution. In the right panel the dashed purple line represents the standard χ PT result and the dashed green line is the combined result. This is to be compared to the blue (red) points that represent the data from Ref. [27] (Ref. [29]).

5 $\gamma\gamma \rightarrow \pi^0\pi^0$ scattering cross section in χ PT $_S$

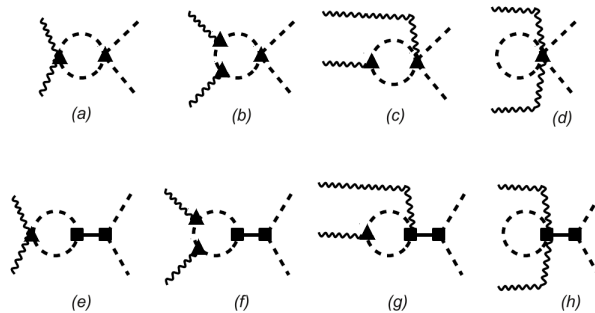


Figure 4: The leading-order diagrams for the process $\gamma\gamma \rightarrow \pi^0\pi^0$ in χ PT $_S$. The upper four correspond to standard χ PT while the lower four appear additionally in χ PT $_S$. The wavy lines are photons. The direction of time is to the right.

There are no $\mathcal{O}(p^2)$ (tree-level) contributions to the reaction $\gamma\gamma \rightarrow \pi^0\pi^0$. Note also that the σ is not charged, so minimal substitution does not generate any tree-level couplings between it and photons. This process therefore must involve pion-loop contributions, and in χ PT $_S$ these come in two varieties: diagrams with a σ pole and diagrams without such a pole.

The top line of Fig. 4 shows the $\mathcal{O}(p^4)$ contributions to the process $\gamma\gamma \rightarrow \pi^0\pi^0$ of the first type. These are the standard χ PT graphs at this order. In χ PT $_S$ the bottom four graphs—again with a dressed σ propagator—are part of the LO amplitude if we consider the region $s \sim M_\sigma^2$.

Before calculating the amplitude for this process we first verify the Ward identity. This states that the scattering amplitude $\epsilon_\mu \Gamma^\mu$ for a process that includes an external photon with a polarization ϵ_μ and momentum k^μ gives zero when the polarization vector of the photon is replaced by its momentum, i.e., $k_\mu \Gamma^\mu = 0$. This holds true for any number of external photons when the associated

polarization vectors are replaced by the corresponding momenta. The Ward identity for the upper four standard χ PT diagrams of Fig. 4 has been verified in Ref. [30]. Here we derive the Ward identity for the bottom four graphs. The general form of the amplitude for these graphs can be written as

$$i\mathcal{T} = i\Gamma \left(\frac{i}{s - m_{S,r}^2 - 2f_{2p,r}s^2 - c_{1d,r}^2 \tilde{\Sigma}(s)} \right) \left(\frac{i2c_{1d,r}(s - 2m_\pi^2)}{F} \right), \quad (10)$$

where $\Gamma = \Gamma_e + \Gamma_f + \Gamma_g + \Gamma_h$ represents the σ -irreducible-vertex for $\gamma\gamma \rightarrow \sigma$ graphs shown in Fig. 5 and the subscripts on each Γ indicate the corresponding diagram. If the vertex Γ obeys the Ward identity then the entire amplitude will obey it.

Suppose $k_{1\mu}$ and $k_{2\mu}$ ($\epsilon_{1\mu}$ and $\epsilon_{2\mu}$) represent the four momenta (polarization vectors) of the external photons of the graphs in Fig. 5 such that $s = (k_{1\mu} + k_{2\mu})^2$. We can verify the Ward identity by replacing either $\epsilon_{1\mu}$ or $\epsilon_{2\mu}$. Here we do it for $\epsilon_{1\mu}$; the result for $\epsilon_{2\mu}$ follows from (1 \leftrightarrow 2) symmetry. Once the replacement $\epsilon_{1\mu} \rightarrow k_{1\mu}$ has been made, the amplitudes $\Gamma_e - \Gamma_h$ are no longer the same. We will call the results of the replacement the *transformed* amplitudes and label them with a superscript W , i.e., $\Gamma_e^W - \Gamma_h^W$.

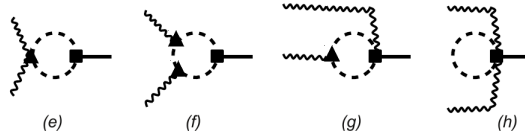


Figure 5: The diagrams that are represented by $i\Gamma$ in Eq. (10).

The sum of the transformed amplitudes corresponding to Fig. 5(e) and Fig. 5(f) can be written as:

$$i\Gamma_e^W + i\Gamma_f^W = \frac{8c_{1d,r}e^2}{F} \left(-\frac{2}{d} \right) \epsilon_{2\nu} k_1^\nu \int \frac{d^4 q}{(2\pi)^4} \frac{q^2}{[q^2 - m_\pi^2]^2}, \quad (11)$$

where d represents the dimension. Similarly, the sum of the transformed amplitudes corresponding to Fig. 5(g) and Fig. 5(h) can be written as:

$$i\Gamma_g^W + i\Gamma_h^W = \frac{8c_{1d,r}e^2}{F} \epsilon_{2\nu} k_1^\nu \int \frac{d^4 q}{(2\pi)^4} \frac{1}{q^2 - m_\pi^2}. \quad (12)$$

Adding up all the transformed amplitudes, employing dimensional regularization, and using $\frac{1}{d} \simeq \frac{1}{4}(1 + \frac{\epsilon}{4})$, we get, as $\epsilon \rightarrow 0$

$$\begin{aligned} i\Gamma^W &= \frac{8c_{1d,r}e^2}{F} \left(-\frac{1}{2} \right) \epsilon_{2\nu} k_1^\nu \frac{i(-m_\pi^2)}{(4\pi)^2} \left[-\frac{4}{\epsilon} - 2 + 2\gamma - 2 \ln \left(\frac{4\pi\mu^2}{m_\pi^2} \right) \right] \\ &\quad + \frac{8c_{1d,r}e^2}{F} \epsilon_{2\nu} k_1^\nu \frac{i(-m_\pi^2)}{(4\pi)^2} \left[-\frac{2}{\epsilon} - 1 + \gamma - \ln \left(\frac{4\pi\mu^2}{m_\pi^2} \right) \right] \\ &= 0. \end{aligned} \quad (13)$$

This verifies the Ward identity.

Turning now to the $\gamma\gamma \rightarrow \pi^0\pi^0$ cross section, the amplitude for the top four standard χ PT graphs of Fig. 4 is evaluated in Ref. [30] and here we simply recycle their results for that part of

the amplitude. Then, the differential scattering cross section for the $\gamma\gamma \rightarrow \pi^0\pi^0$ process in χPT_S can be expressed in the CM frame as

$$\frac{d\sigma}{d\Omega} = \frac{1}{64\pi^2 s} \sqrt{1 - \frac{4m_\pi^2}{s}} \langle |\mathcal{T}|^2 \rangle, \quad (14)$$

where

$$\langle |\mathcal{T}|^2 \rangle = \frac{1}{4} \left(\frac{s^2}{2} + sm_\pi^2 + m_\pi^4 \right) \left(|H_{\chi\text{PT}}(s) + H_\sigma(s)|^2 \right). \quad (15)$$

The standard χPT and additional part of the amplitude that arise in χPT_S ($H_\sigma(s)$) are:

$$H_{\chi\text{PT}}(s) = -\frac{1}{8\pi^2} \frac{2e^2}{F^2} \frac{s - m_\pi^2}{s} \left\{ 1 + \frac{m_\pi^2}{s} \left[\ln \left(\frac{x_+}{x_-} \right) - i\pi \right]^2 \right\}, \quad (16)$$

and

$$\begin{aligned} H_\sigma(s) = & \frac{2c_{1d,r}^2 e^2}{F^2 \pi^2} \left[\frac{1}{4s^2} \left\{ -2m_\pi^2 (s + 2m_\pi^2 \log(m_\pi^2)) + \frac{1}{3} \left(18m_\pi^2 s - 2s^2 + 12m_\pi^4 \log(m_\pi^2) \right. \right. \right. \\ & \left. \left. \left. + 12m_\pi^2 (s - 2m_\pi^2) \left[\text{Li}_2 \left(\frac{1}{x_+} \right) + \text{Li}_2 \left(\frac{1}{x_-} \right) \right] \right\} - \frac{1}{3} \right] \left(\frac{(s - 2m_\pi^2)}{s - m_{S,r}^2 - 2f_{2p,r}s^2 - c_{1d,r}^2 \tilde{\Sigma}(s)} \right), \end{aligned} \quad (17)$$

with x_\pm given by

$$x_\pm = \frac{1}{2} \pm \frac{1}{2} \sqrt{1 - \frac{4m_\pi^2}{s}}. \quad (18)$$

and Li_2 representing the dilogarithm function.

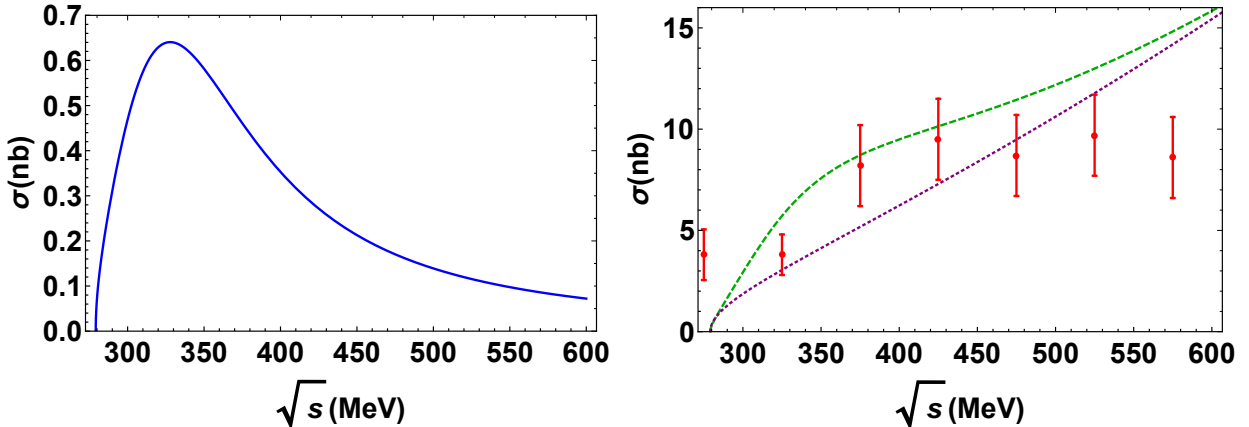


Figure 6: The $\gamma\gamma \rightarrow \pi^0\pi^0$ cross section as a function of the CM energy for $|\cos\theta| \leq 0.8$, where θ is the CM scattering angle. The solid blue (dotted purple) curve represents the contribution from only the bottom (top) graphs of Fig. 4. The dashed green curve is the total combined result. Data from Ref. [31].

The cross-section data for $\gamma\gamma \rightarrow \pi^0\pi^0$ process have been measured by The Crystal Ball Collaboration and reported in Ref. [31]. They analyzed the $e^+e^- \rightarrow e^+e^-\gamma^*\gamma^* \rightarrow e^+e^-\pi^0\pi^0$ reaction from

threshold to about 2 GeV to obtain the cross section. The paper reports that the pion detection efficiency drops considerably for $|\cos\theta| > 0.8$, and therefore they have restricted their extraction of the $\gamma\gamma \rightarrow \pi^0\pi^0$ cross section to the region $|\cos\theta| \leq 0.8$.

Since the differential cross section in Eq. (14) is independent of the scattering angle the total cross section in the region $|\cos\theta| \leq 0.8$ for the $\gamma\gamma \rightarrow \pi^0\pi^0$ process can be written as

$$\sigma = \frac{1}{2} 3.2\pi \frac{d\sigma}{d\Omega},$$

where the factor of 1/2 accounts for the identity of the final-state particles.

In Fig. 6, the left graph shows the $\gamma\gamma \rightarrow \pi^0\pi^0$ cross section due to the lower four graphs of Fig. 4. The result for the total cross section represented by the dashed green curve does have some signal of the σ resonance near 400 MeV. This signal is also slightly visible in the data. Our result for the total cross section agrees with data up to $\sqrt{s} = 450$ MeV. In that energy range it also agrees with the result of Ref. [23] obtained from a Roy-equation treatment of $\gamma\gamma \rightarrow \pi^0\pi^0$.

Refs. [16, 17] obtained good agreement with the $\gamma\gamma \rightarrow \pi^0\pi^0$ and $\gamma\gamma \rightarrow \pi^+\pi^-$ data, respectively. However, they achieved this by adopting a σ -meson propagator

$$\sigma(s) = \frac{1}{s - (M_\sigma - i\Gamma/2)^2} \quad (19)$$

and then adjusting the $\sigma\pi\pi$ coupling that enters the numerator of the σ -pole diagram in $\gamma\gamma \rightarrow \pi\pi$. But unitarity requires that the $\sigma\pi\pi$ coupling is the mechanism by which the width Γ is generated. Ametller and Talavera's approach to the two $\gamma\gamma \rightarrow \pi\pi$ reactions therefore corresponds to a $\pi\pi$ amplitude that is not unitary.

Table 1: The dipole and quadrupole polarizabilities in units of 10^{-4} fm^3 and 10^{-4} fm^5 . The second and third columns contain the standard χPT one-loop and two-loop results from Ref. [30] and Ref. [32] respectively. The fourth column contains the results from dispersion-relation calculations [32]. The last column is our χPT_S result at one-loop.

Polarizabilities	χPT to one-loop	χPT to two-loop	Dispersion relation	χPT_S at one-loop
$(\alpha_1 - \beta_1)_{\pi^0}$	-0.98[30]	-1.9[32]	-1.6[32]	-1.2
$(\alpha_2 - \beta_2)_{\pi^0}$	20.37[30]	37.6[32]	39.7[32]	23.7

Finally, we examine the pion electromagnetic polarizabilities. The stiffness of a pion against deformation by external electromagnetic fields is characterized by dipole and quadrupole polarizabilities. The Compton-scattering reaction $\gamma\pi \rightarrow \gamma\pi$ seems the obvious process from which to extract these quantities, but they can be obtained from $\gamma\gamma \rightarrow \pi\pi$ as well, since the two reactions are related by crossing symmetry. We evaluated the polarizabilities of the π^0 in χPT_S . The values that we obtained for the dipole and quadrupole polarizabilities are presented in Table 1. For comparison purposes, we have also presented the values from standard χPT one-loop [$\mathcal{O}(p^4)$], two-loop [$\mathcal{O}(p^6)$], and dispersion-relation calculations. We see from Table 1 that our calculation does capture some physics beyond the standard one-loop calculation, and seems to incorporate some of the two-loop physics that gives large corrections to both $(\alpha_1 - \beta_1)_{\pi^0}$ and $(\alpha_2 - \beta_2)_{\pi^0}$. However, a calculation with $f_{2p,r} = 0$ (and $c_{1d,r}$ re-adjusted to again reproduce the σ width) bridges half the gap between the $\mathcal{O}(p^4)$ and $\mathcal{O}(p^6)$ polarizabilities. Of course, this is at the cost of an unphysically large $\pi\pi$ and $\gamma\gamma \rightarrow \pi\pi$ cross section.

6 Conclusion

In this paper we have shown that an EFT in which standard χ PT is augmented by the addition of a light scalar field, worked out initially by Soto, Talavera, and Tarrús in Ref. [15], provides a consistent and accurate leading-order description of the σ -meson pole, the isoscalar $\pi\pi$ scattering length, and the data for $\pi\pi$ scattering and $\gamma\gamma \rightarrow \pi^0\pi^0$ up to center-of-mass energies ≈ 500 MeV. This obviates the need for the inconsistent treatment of the $\pi\pi$ amplitude in the latter reaction that was adopted in Ref. [16]. We also found that the analytic result of Refs. [15, 18] for the σ -meson width is too large by a factor of two.

We use a Dyson equation to resum the χ PT_S self-energy correction to the scalar-meson propagator in the vicinity of the resonance. Hence our approach generates a $\pi\pi$ amplitude in the scalar channel that is quite similar to that obtained in the inverse-amplitude method (IAM) [33, 34, 35]. The IAM constructs a unitary $\pi\pi$ amplitude which reproduces both the LO and NLO χ PT results, and (after suitable modification) respects the Adler zero in this channel. However, the IAM does not include a modification to the σ propagator that has it behaving as s^{-2} for s far from the σ pole. The EFT treatment we have adopted here shows that such behavior is, in fact, mandated by the divergence structure of the diagram that generates the leading contribution to the σ 's width in the EFT. The fact that the σ propagator has this unusual off-shell dependence in turn allows the σ to be quite a weak effect once one considers the real energies that are a significant distance from the pole.

An interesting subject for future study would be to explicitly compare the $\pi\pi$ and $\gamma\gamma \rightarrow \pi\pi$ amplitudes obtained in this work and in studies using Roy equations [36, 23] and the IAM [33]. By examining how these amplitudes behave as a function of s as one moves from the σ -meson pole to the real axis where scattering is computed, and then to the sub-threshold region, one could determine the extent to which the simpler amplitude computed here reproduces the features obtained in these more sophisticated approaches.

Lastly, we observe that the power counting in which our leading-order calculation was derived has some issues if its accuracy is reviewed *a posteriori*. For example, the s -channel σ -pole is nominally the LO mechanism [$\mathcal{O}(p^0)$] for $s \sim M_\sigma^2$. However, the results for $\pi\pi$ scattering show that—after all the parameters are chosen—the s -channel σ pole is a fairly small correction to the $\mathcal{O}(p^2)$ χ PT amplitude in this region. Of course, this is because the σ -meson pole has moved so far from the real axis upon the inclusion of the the one-loop self energy. However, that significant movement itself raises concerns, since the power counting employed here is for a narrow resonance, where $i\Gamma/2$ is a perturbative correction to the tree-level mass. It is not clear if the physical σ meson satisfies this criterion. Comparison of the EFT amplitude as a function of s with that found in other approaches will help us understand this issue, since it will illuminate the extent to which the s -dependence of the amplitude arises from the one-loop self-energy effect we have focused on here.

Acknowledgments

We thank Joan Soto, Carlos Schat, and Matthias Schindler for valuable discussions. We are also grateful to Joan Soto for useful comments on the manuscript. This work was supported by the US Department of Energy under grant number DE-FG02-93ER-40756.

References

- [1] J. R. Peláez, Phys. Rept. **658**, 1 (2016) doi:10.1016/j.physrep.2016.09.001 [arXiv:1510.00653 [hep-ph]].

- [2] M. H. Johnson and E. Teller, Phys. Rev. **98**, 783 (1955).
- [3] J. S. Schwinger, Annals Phys. **2**, 407 (1957).
- [4] K. A. Olive *et al.* [Particle Data Group Collaboration], Chin. Phys. C **38**, 090001 (2014).
- [5] I. Caprini, G. Colangelo, and H. Leutwyler, Phys. Rev. Lett. **96**, 132001 (2006) [hep-ph/0512364].
- [6] G. Colangelo, J. Gasser, and H. Leutwyler, Nucl. Phys. B **603**, 125 (2001) [hep-ph/0103088].
- [7] R. Garcia-Martin, R. Kaminski, J. R. Peláez, and J. Ruiz de Elvira, Phys. Rev. Lett. **107**, 072001 (2011) [arXiv:1107.1635 [hep-ph]].
- [8] B. Moussallam, Eur. Phys. J. C **71**, 1814 (2011) [arXiv:1110.6074 [hep-ph]].
- [9] R. A. Briceño, J. J. Dudek, R. G. Edwards and D. J. Wilson, Phys. Rev. Lett. **118**, no. 2, 022002 (2017) doi:10.1103/PhysRevLett.118.022002 [arXiv:1607.05900 [hep-ph]].
- [10] R. J. Crewther and L. C. Tunstall, PoS CD **15**, 132 (2015) [arXiv:1510.01322 [hep-ph]].
- [11] Y. Aoki *et al.* [LatKMI Collaboration], Phys. Rev. D **89**, 111502 (2014) doi:10.1103/PhysRevD.89.111502 [arXiv:1403.5000 [hep-lat]].
- [12] T. Appelquist *et al.*, Phys. Rev. D **93**, no. 11, 114514 (2016) doi:10.1103/PhysRevD.93.114514 [arXiv:1601.04027 [hep-lat]].
- [13] M. Golterman and Y. Shamir, Phys. Rev. D **94**, no. 5, 054502 (2016) doi:10.1103/PhysRevD.94.054502 [arXiv:1603.04575 [hep-ph]].
- [14] D. J. Cecile and S. Chandrasekharan, Phys. Rev. D **77**, 091501 (2008) doi:10.1103/PhysRevD.77.091501 [arXiv:0801.3823 [hep-lat]].
- [15] J. Soto, P. Talavera, and J. Tarrus, Nucl. Phys. B **866**, 270 (2013) [arXiv:1110.6156 [hep-ph]].
- [16] L. Ametller and P. Talavera, Phys. Rev. D **89**, no. 9, 096004 (2014) doi:10.1103/PhysRevD.89.096004 [arXiv:1402.2649 [hep-ph]].
- [17] L. Ametller and P. Talavera, Phys. Rev. D **92**, 074008 (2015) doi:10.1103/PhysRevD.92.074008 [arXiv:1504.06505 [hep-ph]].
- [18] M. Hansen, K. Langble and F. Sannino, Phys. Rev. D **95**, no. 3, 036005 (2017) doi:10.1103/PhysRevD.95.036005 [arXiv:1610.02904 [hep-ph]].
- [19] P. C. Bruns, arXiv:1610.00119 [nucl-th].
- [20] V. Pascalutsa and D. R. Phillips, Phys. Rev. C **67**, 055202 (2003) doi:10.1103/PhysRevC.67.055202 [nucl-th/0212024].
- [21] V. Pascalutsa, M. Vanderhaeghen and S. N. Yang, Phys. Rept. **437**, 125 (2007) doi:10.1016/j.physrep.2006.09.006 [hep-ph/0609004].
- [22] J. A. McGovern, D. R. Phillips and H. W. Griesshammer, Eur. Phys. J. A **49**, 12 (2013) doi:10.1140/epja/i2013-13012-1 [arXiv:1210.4104 [nucl-th]].

- [23] M. Hoferichter, D. R. Phillips, and C. Schat, *Eur. Phys. J. C* **71**, 1743 (2011) [arXiv:1106.4147 [hep-ph]].
- [24] G. Ecker, J. Gasser, A. Pich and E. de Rafael, *Nucl. Phys. B* **321**, 311 (1989). doi:10.1016/0550-3213(89)90346-5
- [25] J. Gasser and H. Leutwyler, *Phys. Rept.* **87**, 77 (1982). doi:10.1016/0370-1573(82)90035-7
- [26] S. Scherer and M. R. Schindler, *Lect. Notes Phys.* **830**, pp.1 (2012). doi:10.1007/978-3-642-19254-8
- [27] J. R. Batley *et al.* [NA48-2 Collaboration], *Eur. Phys. J.* **C70**, 635-657 (2010)
- [28] J. R. Taylor, *Scattering Theory*. John Wiley & Sons, Inc, (1972).
- [29] N. N. Achasov, A. V. Kiselev, and G. N. Shestakov, *Nucl. Phys. Proc. Suppl.* **162B**, 127 (2006) [hep-ph/0605126].
- [30] J. F. Donoghue, B. R. Holstein, and Y. C. Lin, *Phys. Rev. D* **37**, 2423 (1988).
- [31] H. Marsiske *et al.* [Crystal Ball Collaboration], *Phys. Rev. D* **41**, 3324 (1990).
- [32] J. Gasser, M. A. Ivanov, and M. E. Sainio, *Nucl. Phys. B* **728**, 31 (2005). [hep-ph/0506265].
- [33] A. Gomez Nicola, J. R. Peláez and G. Rios, *Phys. Rev. D* **77**, 056006 (2008) doi:10.1103/PhysRevD.77.056006 [arXiv:0712.2763 [hep-ph]].
- [34] C. Hanhart, J. R. Peláez and G. Rios, *Phys. Rev. Lett.* **100**, 152001 (2008) doi:10.1103/PhysRevLett.100.152001 [arXiv:0801.2871 [hep-ph]].
- [35] M. Döring, B. Hu and M. Mai, arXiv:1610.10070 [hep-lat].
- [36] B. Ananthanarayan, G. Colangelo, J. Gasser and H. Leutwyler, *Phys. Rept.* **353**, 207 (2001) doi:10.1016/S0370-1573(01)00009-6 [hep-ph/0005297].